Journal of Southeast University (English Edition) Vol. 26, No. 2, pp. 187 - 191 June 2010 ISSN 1003—7985

Simulation study on combustion system of tankless gas water heater

Qiu Bu[1,2] Zhang Xiaosong[1] Dou Liliang[2]

([1] School of Energy and Environment, Southeast University, Nanjing 210096, China)
([2] A. O. Smith(China) Water Heater Co., Ltd., Nanjing 210038, China)

Abstract: This paper simulates the combustion system of a regular tankless gas water heater under different static pressure conditions. The simulation results are in accordance with the test results. It proves that the used physical and mathematical models are reasonable. The results show that the flame height and the excess air ratios depend on the system pressure drop but not on the absolute pressure at the combustion chamber. The pressure drop and the amount of combustion air have an inverse relationship with CO generation, and they also impact on the temperature and velocity fields. To reduce CO emission, a stronger fan is needed to provide extra pressure head to ensure that enough combustion air is introduced into the system. This study provides a useful research tool to develop products through computational fluid dynamic analysis and laboratory testing.

Key words: tankless gas water heater; combustion system; CO emission; computational fluid dynamics(CFD); static pressure

The tankless gas water heater, an instantaneous hot water supply system, has a wide application in China and Japan. It also has been gaining in popularity compared with the conventional gas storage water heater in the USA[1]. A most common version of such a system today is working with a sealed combustion chamber and a burner group. The burners are set side by side and form spaces between each of the two burners. It is a typical partially-premix combustion system since air flows through the burner and the space between burners. This burner unit is a harmonica-like burner which consists of gas injection, throat tube, venturi and fire ports[2-3].

Traditionally, most of the research work on this type of combustion system has focused on laboratory work and engineering experience. A lot of uncertainty remains and little documentation of research has been found in this particular application field. Lack of computer modeling makes product improvement difficult, since components of a new combustion system are complex and it takes a long time and high expense to obtain a prototype for testing. CFD advances research tools for this system by shortening research time, reducing costs, simulating real or ideal conditions and offering integrated messages[4]. Some CFD and laboratory research have been done recently to present a pollutant emission principle[5-7].

This paper uses CFD to research the combustion system of a tankless gas water heater. A lot of fundamental modeling has been achieved to make this simulation close to a real situation, and some testing has been done for comparison with simulation data.

A typical tankless gas water heater, as shown in Fig. 1, is modelled in 3D. The main air stream is separated into primary air and secondary air since it is fanned into the system from an air inlet. Primary air flows into the combustion chamber through the burner and secondary air flows into the combustion chamber through gaps between the burners. The fuel, which is methane from a nozzle in this case, jets into the inlet of the burner and mixes with the primary air. Most of the fuel-air mixture jets into the combustion chamber through the burner outlet and combusts, forming a short inner flame. This flame, known as premix flame, is a fuel-rich flame. A small portion of the fuel-air mixture passes the flame stabilization holes and combusts between the flame stabilization plates to stabilize a premix flame. The excess fuel, or rather the fuel-related intermediate species, passes through the premix flame and reacts with the secondary air to form a non-premixed flame. These flames form a Bunsen flame[8].

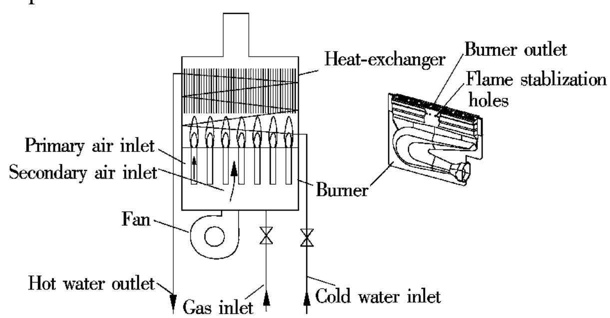

Fig. 1 Principle of a typical tankless gas water heater combustion system and its burner

1 Methodologies

1.1 Physical models

A 3D model of parts of a tankless gas water heater is established to avoid huge computational time and maintain accurate results. The unstructured mesh is created based on this physical model.

This paper researches the velocity, the temperature and the CO emission of this system at different outlet static pressures, 0, 50, 100, and 150 Pa, in order to simulate different lengths of flue pipes. The high static pressure may also come from an instant strong wind from the outside or the downstream secondary heat exchanger. So, in this case, an extreme condition at 1 kPa is also studied.

The finite-rate/eddy-dissipation species transport and reaction model, which computes both the Arrhenius rate and the mixing rate and uses the smaller of the two, is chosen to simulate reaction.

In order to predict CO emission, a three-step chemical reaction model is adopted as follows:

Received 2009-11-17.

Biographies: Qiu Bu (1972—), male, graduate; Zhang Xiaosong (corresponding author), male, doctor, professor, rachpe@seu.edu.cn.

Citation: Qiu Bu, Zhang Xiaosong, Dou Liliang. Simulation study on combustion system of tankless gas water heater[J]. Journal of Southeast University (English Edition), 2010, 26(2): 187 - 191.

$$\left.\begin{array}{l} CH_4 + 1.5O_2 \rightarrow CO + 2H_2O \\ CO + 0.5O_2 \rightarrow CO_2 \\ CO_2 \rightarrow CO + 0.5O_2 \end{array}\right\} \quad (1)$$

The turbulence model is the standard k-ε model, which is the simplest "complete model" of turbulence models. It is an economical and reasonablely accurate turbulence model for this case. The standard wall function, which has been most widely used for industrial flows, is used for this case. And the discrete ordinates(DO) model is chosen as the radiation model.

1.2 Boundary condition

The gas inlet pressure is the one after the gas valve and at the gas tube near the nozzle, and is set at a fixed value. The air inlet pressure is mainly related to the characteristics of the system and the fan, here set as an input data for CFD calculation. The air inlet pressure indicates the pressure starting point of the primary air. The pressure head of the total air system depends on the fan' s output power.

The outlet flue gas pressure is defined as the pressure at the flue outlet to obtain a better rate of convergence.

In order to research how the pressure at the flue outlet influences the system performance, boundary conditions are set as shown in Tab. 1.

Tab. 1 Boundary conditions in different cases Pa

Case	Flue outlet pressure	Air inlet pressure	Gas inlet pressure
CFD-1	0	200	1 000
CFD-2	50	200	1 000
CFD-3	100	200	1 000
CFD-4	150	200	1 000
CFD-5	150	350	1 000
CFD-6	1 000	1 200	2 000

2 Results and Discussion

We choose the burner central plane XY along its length direction as the research plane for easy analysis.

2.1 Velocity magnitude at XY section at different flue outlet static pressures

Fig. 2 shows the details of the velocity distributions at the XY section in cases CFD-1 to CFD-6. It is clearly a pressure-dependent velocity distribution. The maximum velocity magnitudes of these six cases are all at burner outlet ports. There is a greater velocity gradient at the interface of two burners than at any other points of the section, and this velocity gradient results in some long and strait isolines especially when the flue outlet static pressure is 0 Pa. This results in different flame structures for cases CFD-1 to CFD-5. And it is found that the velocity gradient influences air communication between premix flame and non-premix flame. Control of these velocity isolines is important for flame stabilization. Exorbitant velocity will bring on the flame lifting and too low velocity will make the flame flash back.

The velocity fields of cases CFD-1 and CFD-6 are almost the same. There is a conclusion that the pressure drop instead of the absolute pressure value dominates the velocity fields. And we will obtain similar results in the following temperature and CO concentration fields.

The curves at the top of Figs. 2 (a) to (f) show the temperature distributions at the top of the combustion chamber or at the bottom of the heat exchanger. The notable velocity gradient is presented, because the air and gas mixture releases

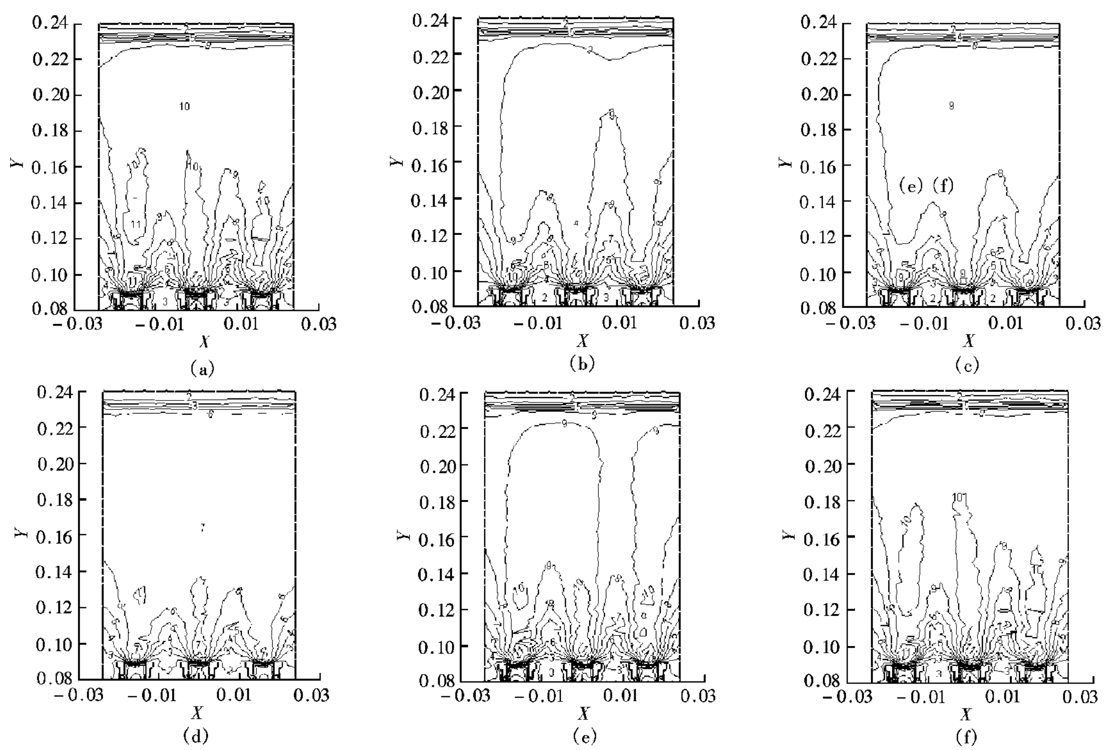

1—0 m/s;2—0.6 m/s; 3—1.1 m/s;4—1.7 m/s; 5—2.3 m/s;6—2.9 m/s; 7—3.4 m/s;8—4.0 m/s; 9—4.6 m/s;10—5.1 m/s; 11—5.7 m/s;12—6.3 m/s; 13—6.9 m/s;14—7.4 m/s; 15—8.0 m/s

Fig. 2 Velocity magnitude at XY section at different outlet static pressures. (a) Case CFD-1; (b) Case CFD-2; (c) Case CFD-3; (d) Case CFD-4; (e) Case CFD-5; (f) Case CFD-6 the energy and the temperature decreases dramatically. And, hence, the mixture velocity decreases since the mass is constant and the section area does not change.

2. 2 Temperature distributions at *XY* section at different flue outlet static pressures

Fig. 3 shows the details of the temperature distributions at the *XY* section. The isolines of the temperature distributions are similar to those of the velocity distributions because the balance of the mixture velocity and the reaction velocity determines the structure of the flame. Researching the velocity field without combustion is important since it is easy and approximately accurate. However, the temperature field research is still meaningful. The highest temperature isoline 14, which represents the reaction centres, is almost at the same height except in Figs. 3(c) and (d).

Figs. 3(c) and (d), in which the high temperature isolines cover most parts of the figures, indicate some poor combustion situations. The air excess ratio of these two cases is too low to provide enough air to combust all the fuel and oxidize CO to CO_2. The temperature isolines of cases CFD-1 and CFD-6 are the same as the velocity isolines because of the same pressure drop.

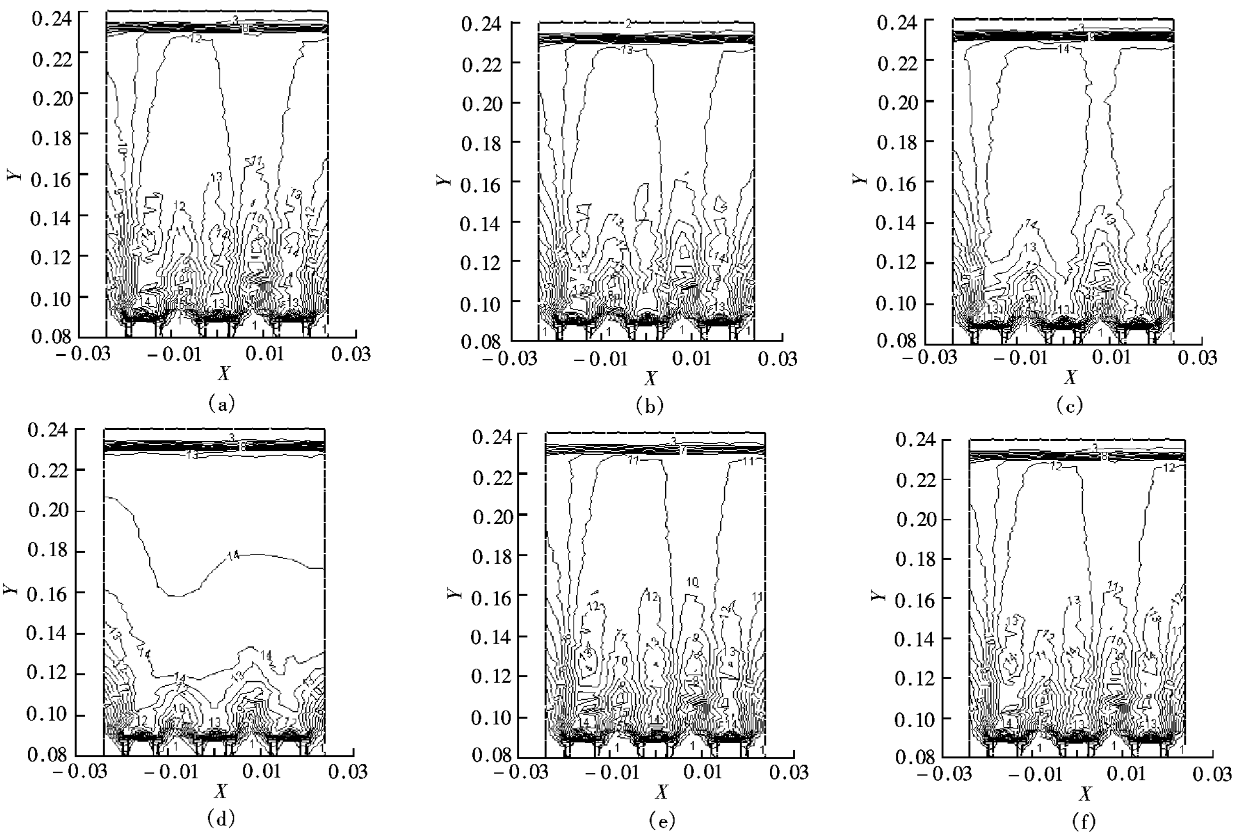

1—300 K; 2—436 K; 3—571 K; 4—707 K; 5—843 K; 6—979 K; 7—1 114 K; 8—1 250 K; 9—1 386 K; 10—1 521 K; 11—1 657 K; 12—1 793 K; 13—1 929 K; 14—2 064 K; 15—2 200 K

Fig. 3 Temperature distributions at *XY* section at different flue outlet static pressures. (a) Case CFD-1; (b) Case CFD-2; (c) Case CFD-3; (d) Case CFD-4; (e) Case CFD-5; (f) Case CFD-6

2. 3 CO concentration at *XY* section at different flue outlet static pressures

Fig. 4 shows the CO concentration field. In Fig. 4(a), isoline 2, which represents the lowest CO concentration less than 36×10^{-6}, indicates that the reaction is quicker than that of any other cases. Case CFD-2 in Fig. 4(b) is also a good case, although it has a CO concentration higher than that of Fig. 4(a). Case CFD-4 in Fig. 4(d) is an extreme one, in which the CO level is very high, meaning most parts of the chamber are in lack of air.

However, because inlet air pressure increases when the outlet flue gas pressure increases, cases CFD-5 and CFD-6 still perform well at CO emission. The case CFD-5 is the best one since its gas input is less than that of the others. The pressure difference between the primary air and the gas inlet is smaller, so this means that less gas is introduced from the gas nozzle into the burner.

The air excess ratio is an important design factor in a non-premix combustion system. In some given systems with different gas flue pipes, they are mainly influenced by introduced air volume. In this case, it keeps dropping when flue outlet static pressure increases. Fig. 5 shows this tendency and the tendency of the CO emission in cases CFD-1 to CFD-4. To avoid high CO emission in these poor cases, we need to provide a higher output fan to supply more air and to increase air excess ratios. This conclusion is proved to be right by laboratory testing as shown in Tab. 2. We test a system as shown in Fig. 1 at different fan speeds. The results show that CO emission linearly decreases with the increase in fan speed.

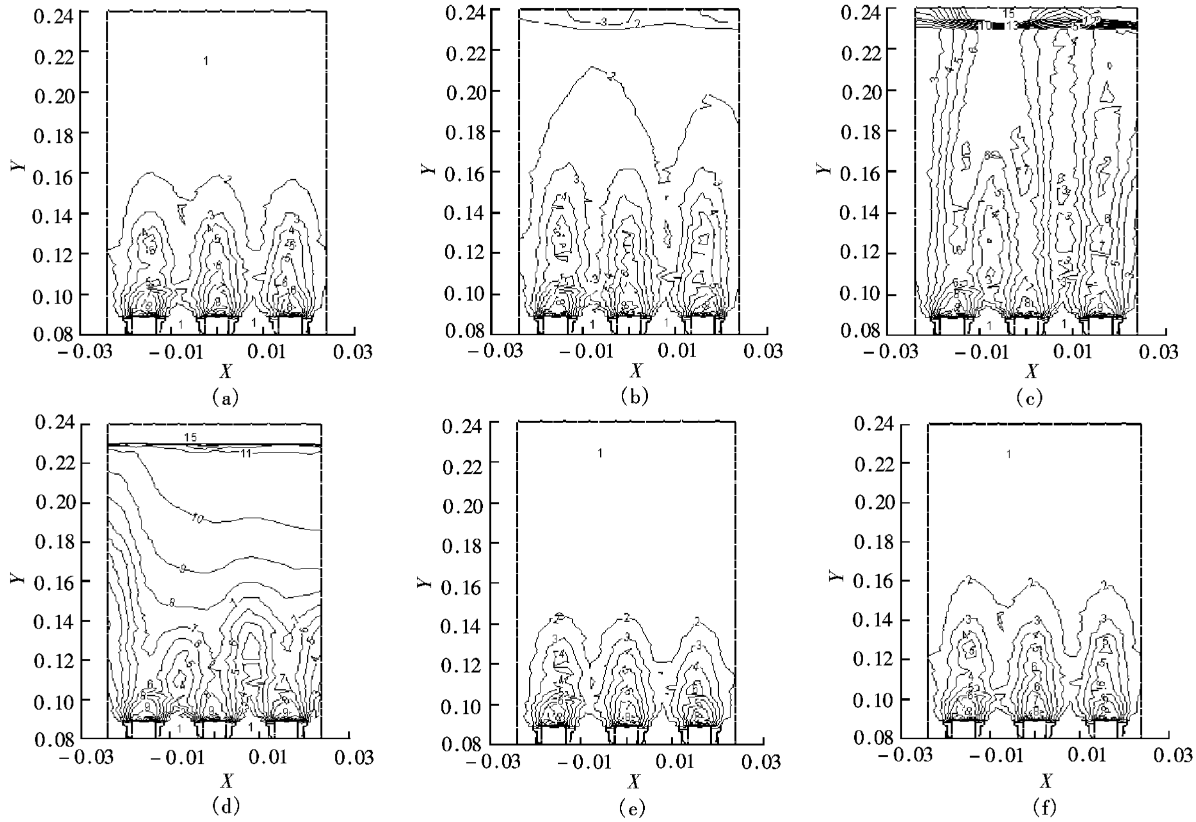

1—0 ;2—36 × 10^{-6}; 3—71 × 10^{-6};4—107 × 10^{-6}; 5—143 × 10^{-6}; 6—179 × 10^{-6}; 7—214 × 10^{-6}; 8—250 × 10^{-6}; 9—286 × 10^{-6};10—321 × 10^{-6}; 11—357 × 10^{-6};12—393 × 10^{-6}; 13—429 × 10^{-6}; 14—464 × 10^{-6}; 15—500 × 10^{-6}

Fig. 4 CO concentration fields at *XY* section at different flue outlet static pressures. (a) Case CFD-1; (b) Case CFD-2; (c) Case CFD-3; (d) Case CFD-4; (e) Case CFD-5; (f) Case CFD-6

Tab. 2 Testing data of CO emission and air excess ratios at different pressure drops

Case	DC fan speed/ ($r \cdot min^{-1}$)	Outlet flue gas pressure/Pa	Inlet air pressure/Pa	Gas pressure/Pa	CO emission/ 10^{-6}	Air excess ratio
Lab-1	5 400	0	174	1000	86	2. 55
Lab-2	5 200	26	190	1000	202	2. 32
Lab-3	5 000	69	202	1000	535	1. 53

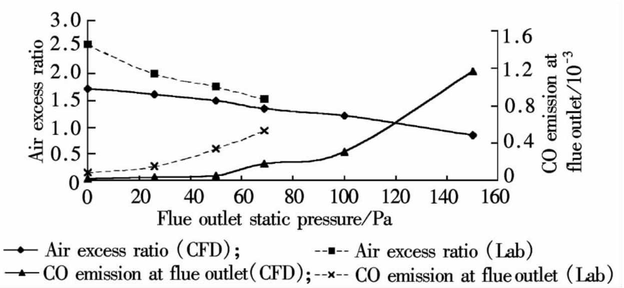

Fig. 5 CO concentration at flue gas outlet and air excess ratio at different flue outlet static pressures

We test three cases of a tankless water heater system, without flue, with a standard flue and with a 5 m length flue and three elbows. Fig. 5 shows that the CFD analysis predicts the same tendency as the test results.

2. 4 Static pressure at different height sections of water heater at different outlet static pressures

Fig. 6 shows the static pressure at different height sections in the testing of cases Lab-1 to Lab-3. Fig. 6 also presents the static pressure at the same height section by the CFD of cases CFD-1 to CFD-5, indicating that CFD predicts a good tendency of CO emission and air excess ratios changing at different inlet air pressures as laboratory testing does.

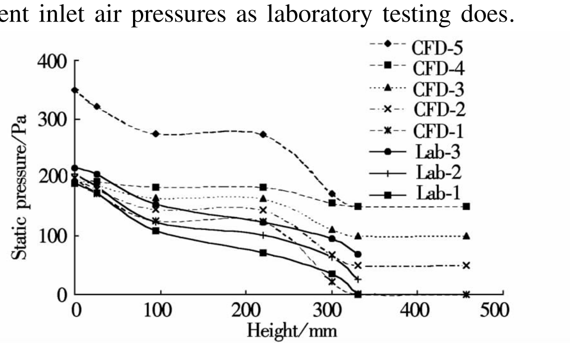

Fig. 6 Static pressure at different height sections of water heater at different outlet static pressures

3 Conclusions

1) Simulation provides engineers and researchers abundant useful information such as velocity, temperature and carbon monoxide.

2) The physical and mathematical models presented in this

paper are capable of simulating combustion phenomena and the CO emission of a tankless gas water heater, and they give directions for improvement.

3) A typical Bunsen flame is simulated in this paper. The flame height and air excess ratios depend on the flue outlet static pressure under a given air inlet condition.

4) The CO emission also depends on the flue outlet static pressure in a given system. To reduce CO emission, a stronger fan is needed to provide an extra pressure head to ensure that enough combustion air is introduced into the system. There is a chance of optimization by adjusting the ratio of primary air to secondary air as well as gas inlet pressure.

References

[1] Dieckmann J, McKenney K, Brodric J. Gas tankless water heaters[J]. *ASHRAE Journal*, 2009, **51**(12): 117 − 118.

[2] Rinnai Corporation. Gas burner: Japan H02-100018U [P]. 1990.

[3] Noritz Corporation. Impact forging forming metal combustor and method for producing the same impact forging metal combustion device: China, 03155304. 4A[P]. 2005. (in Chinese)

[4] Patankar S V. *Numerical heat transfer and fluid flow* [M]. Washington DC: Hemisphere Publishing Corp, 1980: 4 − 5.

[5] Huang S, Peng S N, Luo X C, et al. Numerical simulation of combustion and pollutants emission about instantaneous gas water heater [J]. *Energy Engineering*, 2007(1): 48 − 52. (in Chinese)

[6] Zhang J. Gas water heater status of the different combustion laboratory tests and analysis [J]. *Shanghai Measurement and Testing*, 2008(3): 41 − 43. (in Chinese)

[7] Yang J. Numerical analysis of the fan instantaneous gas water heat' chamber [D]. Wuhan: School of Environmental Science and Engineering, Huazhong University of Science and Technology, 2006. (in Chinese)

[8] Law C K. *Combustion physics* [M]. New York: Cambridge University Press, 2006: 265 − 266.

快速式燃气热水器燃烧系统模拟

邱　步[1,2]　张小松[1]　窦礼亮[2]

([1] 东南大学能源与环境学院,南京 210096)

([2] A. O. 史密斯(中国)热水器有限公司,南京 210038)

摘要:模拟了一种常规快速式燃气热水器的燃烧系统,研究了不同压力状况下的燃烧工况. 得到的数值模拟结果与实验获得的数据吻合得较好,证明了所用物理模型和数学模型的合理性. 结果显示,火焰高度和过剩空气系数依赖于系统出口和入口的静压差,而与燃烧室内的绝对压力无关. 该静压差和系统中用于燃烧的空气量显著影响 CO 的生成,与 CO 的生成量呈反比关系,并同时影响燃烧区域内的温度场和速度场. 为降低 CO 排放水平,必须增加进入燃烧系统的空气量,因此需要增加风机输出功率以提供足够的空气压头. 该研究为设计快速式燃气热水器提供了一种行之有效的方法.

关键词:快速式燃气热水器;燃烧系统;CO 排放;计算流体动力学;静压

中图分类号:TK16